

Absorption measure distribution (AMD) measures the distribution of absorbing column over a range of ionization parameters of the X-ray absorbers in Seyfert galaxies. In this work, we modelled the AMD in Mrk 509 using its recently published broad band spectral energy distribution (SED). This SED is used as an input for radiative transfer computations with full photoionization treatment using the photoionization code *Titan*. We show that only for the warm absorber being the cloud under constant total pressure (gas+radiation), we are able to reproduce the discontinuities in the observed AMD. Such dips were thought to be described due to thermal instabilities, but our work shows it clearly for the first time.

Introduction

Based on high resolution X-ray data, there is a general consensus that the majority of Seyfert galaxies contain the ionized absorbing gas in their line of sight. X-ray instruments like Chandra, XMM-Newton and Suzaku provided great opportunity for the extensive studies of the absorbing gas, so called warm absorber (hereafter WA) in AGNs. These studies were done on the basis of narrow absorption lines from highly ionized elements, observed with the use of gratings. Since then, many attempts were made exploring the ionization structure of the WA in several AGNs (Holczer, Behar & Kaspi 2007; Behar 2009; Detmers et al. 2011).

Holczer, Behar & Kaspi (2007) introduced the term Absorption Measure Distribution (AMD) to quantify the absorption strength and the ionization structure on the basis of observed ionic column densities from the absorption lines seen in the high resolution X-ray spectra. They have shown that, in case of the source IRAS 13349+2438, AMD has deep minimum in column density around the ionization parameter between $\log(\xi) \sim 0.8$ and 1.8. Such deep minima are present in AMD of other objects as well and they are interpreted as the observational evidence for thermal instability in a given ionization and temperature regime. The ionization and temperature regime at which these discontinuities occur may also depend on the shape of the incident continuum as inferred from the fact that the stability curve strongly depends on the SED (Różańska, Kowalska & Gonçalves 2008; Chakravorty et al. 2009). Most recently, Stern et al. (2014) successfully reproduced the continuous AMD structure for Seyfert galaxies assuming the radiation pressure confinement (RPC) of the absorbing material. However, they were not able to reproduce and explain the observed discontinuity in their modelled AMD. In this work, we show that if the gas is in total pressure equilibrium, the observed discontinuity in AMD structure can be reproduced and agrees well with the observations for the case of Mrk 509 Sy 1 galaxy. For this purpose, we use photoionization code *Titan* (Dumont, Abrassant & Collin 2000), which fully takes into account the radiation pressure stratification computed at each zone from radiation intensity.

Our model

We considered the absorbing gas is in total pressure equilibrium which self consistently allows it to be stratified in density when illuminated by the SED. We used the code *Titan* (Dumont, Abrassant & Collin 2000) for computing the photoionization and hence determining the structure of the warm absorber. Photoionization code solves the full radiative transfer equation and the physical state of the gas at each depth is determined assuming the local balance between ionizations and recombinations of ions, excitations and de-excitations, local energy balance and finally total energy balance. The photoionization modelling requires at least the input parameters: SED, hydrogen number density, ionization parameter (all defined at the illuminated side of the cloud) and chemical composition. In our model, we considered a plane parallel slab of gas with solar composition illuminated by a well constrained SED of Mrk 509 (Fig. 1, red circles) adopted from Kaastra et al. 2011. Photoionization code accepts an input SED as points and interpolates linearly, if needed. Therefore, incident spectrum fully agrees with observed broad-band continuum (Fig. 1 black line)

The ionization parameter at the illuminated side of the cloud is defined as

$$\xi_0 = L/n_0 r^2 \quad (1)$$

where L is hydrogen ionizing luminosity, n_0 is hydrogen number density at the illuminated side and r is the distance to the absorber from the ionizing source. The ionization parameter at each depth can be expressed in terms of radiation pressure and gas pressure as

$$\xi(z) = 4\pi c k T(z) P_{\text{rad}}(z) / P_{\text{gas}}(z) \quad (2)$$

$$= 4\pi c k T(z) \Xi(z) \quad (3)$$

where Ξ is dynamical ionization parameter and z is geometrical depth

The AMD is computed as

$$\text{AMD} = dN_{\text{H}} / d(\log \xi) \quad (4)$$

where dN_{H} is the column density at each layer of the slab. The AMD distribution versus ionization parameter ξ , measured from observations is model dependent. In particular, it takes ionic column densities computed for maximal ξ responsible for the given ionization state of the particular ion. In reality, total ionic column densities should be computed from some distribution of ξ over several layers. Therefore, our fully consistent model slightly over predicts the resulting normalization of AMD, but it reproduces exactly two dips observed in case of Mrk 509. This is strong evidence, for the warm absorber being under constant pressure rather than constant density.

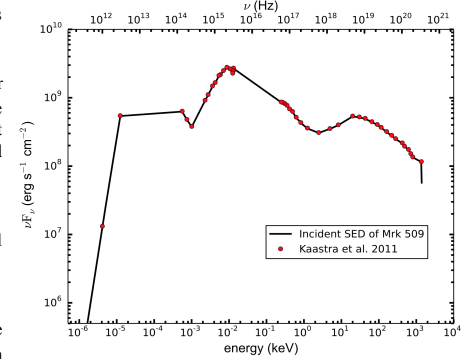


Fig. 1 SED of Mrk 509 taken from Kaastra et al. 2011

Stability Curve (log(T) vs log(Ξ))

The stability curves computed from *Titan* agree with those computed by publicly available code CLOUDY (Ferland et al. 2013) with the assumption of constant density and constant pressure are shown in Fig. 2 (a) and Fig. 2 (b) respectively. For these calculations, we considered the hydrogen ionizing luminosity of Mrk 509 to be 3.2×10^{45} erg s⁻¹ and the inner radius of the absorber $\log(r/\text{cm}) = 17.25$. For a constant density approximation, we require a grid of constant density clouds to fully reproduce the stability curve except for the case with extended envelopes (spherical geometry). In case of extended envelopes, the radiation pressure changes going deeper into the cloud due to geometrical dilution and absorption by ionized gas and it is possible to get a full stability curve.

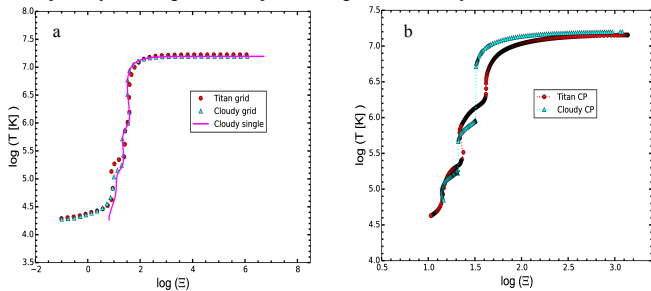


Fig. 2 (a) Stability curves for constant density plane parallel clouds using *Titan* (red circles) and *Cloudy* (cyan triangles). Each point in both cases represent the single cloud with the grid in density range $\log(n_0/\text{cm}^{-3}) = 2-12$. Magenta line shows stability curve for the constant density single cloud with spherical geometry obtained from *Cloudy*. (b) Cooling curve obtained from *Cloudy* (cyan triangles) and *Titan* (red circles) for the case of absorbing medium under constant pressure. Both the curves are produced with the number density $n_0 = 10^6$ cm⁻³ and ionization parameter $\xi_0 = 10^6$ erg cm s⁻¹ at the irradiated surface of the cloud. The inner radius to the cloud is set to 5.656×10^{16} cm. The total column density (N_{H}) of the slab in both calculation is set to 1.5×10^{23} cm⁻².

As we can see from the Fig. 2 (a), all the curves agree down to the temperature 3×10^4 K. We are more interested in constant pressure clouds since this assumption provides us the continuous structure for AMD with two dips, which can not be obtained in the case of RPC cloud as shown by Stern et al. (2014). As shown in Fig. 2 (b), the constant pressure cooling curves from *Cloudy* and *Titan* shows the similar trend except for the considerable difference in the thermal instability zone. Thermal instability zones are part of the stability curve where the slope is negative. The main difference between two codes here is that *Cloudy* is not able to compute the structure at the zones of instability. Also there is a difference in the range of ionization parameter at which the instability occurs. This difference may be due to the different approximations used in the code to solve thermal balance equation and the differences in the atomic database used.

References

- Behar E., 2009, *ApJ*, 703, 1346
 Chakravorty S., Kembhavi A. K., Elvis M., Ferland G., 2009, *MNRAS*, 393, 83
 Detmers R. G. et al., 2011, *A&A*, 534, A38
 Dumont A.-M., Abrassant A., Collin S., 2000, *A&A*, 357, 823
 Ferland G. J. et al., 2013, *Rev. Mexicana Astron. Astrofis.*, 49, 137
 Holczer T., Behar E., Kaspi S., 2007, *ApJ*, 663, 799
 Kaastra J. S. et al., 2011, *A&A*, 534, A36
 Różańska A., Kowalska I., Gonçalves A. C., 2008, *A&A*, 487, 895
 Stern J., Behar E., Laor A., Baskin A., Holczer T., 2014, *MNRAS*, 445, 3011

Results & Discussion

AMD for Mrk 509

AMD as defined in eq. (4), measures the distribution of the absorption strength at all depths throughout the cloud. In most of the cases, observations show that there exists a large range of ionization states at a different distances from the source along the line of sight (Holczer, Behar & Kaspi 2007; Behar 2009; Detmers et al. 2011). Detmers et al. (2011) derived the observational AMD for Mrk 509 using 600 ks RGS spectrum and they found two discontinuities in the regime of $\log(\xi)$ between 2.4 and 2.8 and between 3.5 and 4.0. These thermally unstable regions can be clearly seen in Fig. 2 (b) (curve presented with red circles) occurring in the temperature regime between $\log(T/\text{K}) = 5.3 - 6.5$. These regions correspond to the dips in the AMD as shown in Fig 3 (a), which agrees with the observational results obtained by Detmers et al. (2011). The locations of the dips do not agree exactly but the range of ionization parameter agrees. The observational AMD is also model dependent as hydrogen column density can not be obtained directly from observation. Usually, hydrogen column density is derived using the ionic column densities obtained by fitting the absorption lines using photoionization models. Nevertheless, with our assumption of an absorber under total pressure equilibrium, it is possible to explain the distribution of the absorbing column as well as the discontinuities seen in the observation.

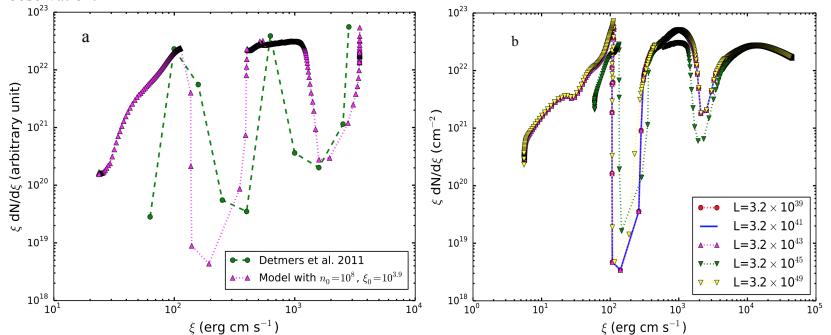


Fig. 3 (a) Comparison between the observational AMD (green circles) from Detmers et al. (2011) and AMD obtained using our model (magenta triangles) of an absorber under constant pressure for the case of model parameters shown in the plot. (b) AMD for the different source luminosities and the density $n_0 = 10^6$ cm⁻³. (c) AMD for $n_0 = 10^6$ cm⁻³ and different cases of ionization parameters at the illuminated side of the cloud considered.

We also found that, considering different values of source luminosity does not significantly change the AMD behaviour as seen in Fig. 3 (b). Fig. 3 (c) illustrates the AMD for different cases of ionization parameter ξ_0 and $n_0 = 10^6$ cm⁻³ at the illuminated side of the slab of gas. It is clearly seen from the figure that varying ξ_0 only changes the normalisation in the AMD vs $\xi(z)$ plot.

Acknowledgements: We want to thank J. S. Kaastra for providing us the SED of Mrk 509, we used in our study. This research was supported by Polish National Science Centre grants No. 2011/03/B/ST9/03281, 2013/08/A/ST9/00795, and by Ministry of Science and Higher Education grant W30/7.PR/2013. It received funding from the European Union Seventh Framework Program (FP7/2007-2013) under grant agreement No.312789.